

AN EXAMINATION OF THE EFFECTS OF
STRONG ELECTRIC FIELDS ON
SUPERCOOLED WATER DROPS

A Thesis
Presented to the Graduate Faculty of the
New Mexico Institute of Mining and Technology

In Partial Fulfillment
of the Requirements for the Degree
Master of Science
in Geophysics

by
Evan L. Ausman, Jr.
June 1963

TABLE OF CONTENTS

	Page
ABSTRACT -----	1
ACKNOWLEDGEMENTS -----	3
INTRODUCTION -----	4
THEORY -----	6
APPARATUS -----	14
Refrigerator -----	14
Temperature Measurement -----	15
Water Droppers -----	17
Precooling Bath -----	18
Field Plates and Electric Field -----	19
Corona and Spark Detectors -----	20
Photography -----	21
Pressure Measurement -----	23
OBSERVATIONS -----	26
SUMMARY AND CONCLUSIONS -----	32
SUGGESTIONS FOR FURTHER INVESTIGATION -----	35
APPENDIX -----	36
Table 1, Summary of Primary Observations ---	37
Table 2, Drop Temperature, Corona Field, and Spark Field -----	40
Table 3, Percent Difference Between Highest and Lowest Values of Field at Constant Temperature -----	43
Table 4, Distortion of 0.21 Cm. Radius Drop	44

Table 5, Surface Tension of Water vs. Temp.	45
Results of Calorimeter Check of Ludlam's Equation -----	46
Calculation of Expected Error in Drop Radius	47
Table 6, Expected Errors of Measurements --	48
Table 7, Values of Field Calculated From NACA Standard Atmospheric Pressures and Temperatures -----	49
BIBLIOGRAPHY -----	50

ILLUSTRATIONS

Figure No.		Page
1	Photograph of Refrigerated Drop Tower -----	16
2	Flash Circuit Diagram -----	22
3	Photograph of a Water Drop in its Corona Field --	24
4	Corona Field Vs. Drop Temperature -----	27
5	Sparking Field Vs. Drop Temperature -----	29
6	Field Vs. Distortion Ratio -----	31

ABSTRACT

A refrigerated drop tower was constructed and used to cool water drops as they fell through the air. The drops passed into a region of high electric field. Observations were made of the distortion, corona onset, and sparking fields for different drop radii (0.13 cm. to 0.22 cm.) and temperatures (29.2 degrees C. to -9 degrees C.). Room temperature observations agreed well with those of Macky.

It was observed that a decrease in temperature causes an increase in the corona and sparking fields for a given drop radius. The increase in the corona field, for drops of radius 0.15 cm., from +20 degrees Centigrade to -9 degrees Centigrade is about 13%. A 3% increase in the corona field was calculated from Macky's formula using the variation of the surface tension of water with temperature over the same range. Macky's values for corona field must be corrected for temperature if they are to be applied to the natural environment within thunderstorms.

No nucleation of the water drops was observed at temperatures as low as -9 degrees Centigrade.

An empirical equation, based on Macky's equation for the corona field, taking the temperatures into account, and calculated for the observations is:

$$E = 447 \frac{(75.6 + 8.8 - 0.77T + 0.0039 T^2)^{\frac{1}{2}}}{(r)^{\frac{1}{2}}},$$

where T is the water drop temperature in degrees Centigrade,
 E is in v/cm., and r is in cm.

AN EXAMINATION OF THE EFFECTS OF STRONG ELECTRIC FIELDS ON SUPERCOOLED WATER DROPS

INTRODUCTION

An examination of the effects of strong electric fields on supercooled water drops was of special interest because of their possible relationship to the thunderstorm charge generation mechanisms and to initiation of lightning discharges.

The primary conditions which affect water drops in a thunderstorm cloud are: pressure, temperature, electric charges (both free and induced), strong electric fields,

and type of contamination of the water.

This thesis is concerned with the electric field necessary to cause corona to be emitted from freely falling water drops of different radii and temperatures.

The breakdown field for dry air at N.T.P. is 30,000 volts per centimeter. W. A. Macky (1931) found that this field was reduced to 8,000-10,000 volts per centimeter when water drops were present. Macky studied the variation of corona and sparking fields for different drop sizes and reduced pressure. It must be assumed that his experiments were carried out at room temperature since no temperatures were given. Macky used 75.0 dynes per cm. as the surface tension of water in his empirically derived equation for the field and assumed that it was a constant. The surface tension of water increases with a decrease in temperature, (Table 5). The author, therefore, re-examined freely falling water drops in strong electric fields to observe the effect of temperature on the corona and sparking fields.

THEORY

Mackay (1931) showed that water drops emit a fine spray of tiny droplets when subjected to strong electric fields. He examined the effects of increased fall velocity and reduction of air pressure. Ever since the early work of Mackay on the lowering of the breakdown potential gradient in air produced by the presence of water drops, it has been assumed, for the purposes of computation of maximum charge containment, that the breakdown electric field in thunderstorm clouds is between 8,000 and 10,000 volts per centimeter.

Consider a water drop in a uniform electric field E_0 . The surface tension forces are counteracted by the electrical stress on the surface of the drop. This stress may be due to induced charge, free charge, or both. By equating the surface tension force on the circumference of a drop to the force due to the internal pressure on the cross-sectional area of the drop, we obtain; $2 \pi r S = \pi r^2 P$, $P = 2 S/r$. P represents internal pressure of the drop, S , the surface tension, and r , the radius. The stress on the surface of the drop due to a charge on it is $\frac{\sigma^2}{2\epsilon_0}$, where σ is the surface charge density at a point. A drop may be expected to breakup when the surface tension stress, $P = 2 S/r$, is equal to the electrical stress, $\frac{\sigma^2}{2\epsilon_0}$, at any point on the surface. The induced surface charge, σ , on a drop in a strong electric field may be calculated from $E_s = \frac{\sigma}{\epsilon_0}$ at the surface

of a conductor because the field within a conductor is zero. The relaxation time of water is approximately equal to 10^{-6} seconds. A water drop is therefore considered a good conductor.

The field at the surface of a spherical drop in a uniform field is,

$$E_s = 3 E_0 \cos \theta.$$

From this, $E_m = 3 E_0$ when θ equals zero, the maximum field at the surface of the drop.

The field, E_d , that was obtained from the above stress equation is,

$$E_d = 2 (S / \epsilon \cdot r)^{1/2} \text{ in mks units, or}$$

$$E_d = 6720 (S/r)^{1/2},$$

where S is in dynes per cm., r is in cm., and E_d is in volts per centimeter.

Equating the maximum field, E_m , at the surface of a drop in a uniform field to the field, E_d , necessary to overcome surface tension forces, we obtain;

$$E_0 = 2240 (S/r)^{1/2}.$$

E_0 is the applied field in volts per centimeter. This represents the theoretical value of the applied field which should cause disruption of a spherical drop of radius r . Since the drops are distorted by the field, they are no longer spherical and this formula is not expected to apply.

According to Loeb (1953), Macky's "observations indicated that, as fields reached intensities of the order of 7-8 kv/cm,

water drops, depending on their size, began to be drawn out into spindle shaped configurations, the ends of which broke into sharp points and fine spray, accompanied by visible corona discharge. This action indicates that in high electric fields water drops distort, disrupt, and discharge negative and positive ions into the gas by means of point coronas." From Loeb's description it is assumed that as a water drop disrupts it emits corona. Therefore, the applied field, E_0 , which causes disruption is assumed to be the same as the field which causes corona emission.

The surface tension of water is tabulated in Table 5 as a function of temperature. It is expected, on the basis of surface tension alone, that the breakdown field would be a function of temperature if the surface tension forces are overcome before the breakdown field for air is reached. According to this theory, a surface tension change from 72.0 dynes per cm. at 25 degrees Centigrade to 76.4 dynes per cm. at -5 degrees Centigrade gives an increase in field of 3% for a given drop radius.

A nucleated water drop was expected to give much higher values of corona and sparking fields than those observed for water drops due to the hindrance to distortion and disruption by the ice. However, no nucleation of the water drops was observed down to temperatures as low as -9 degrees Centigrade.

Mackay derived an empirical formula,

$$E_{\text{corona}} = 447 \left(\frac{S}{r} \right)^{\frac{1}{2}}$$

E corona is the corona field in volts per centimeter, surface tension is in dynes per centimeter, drop radius is in centimeters. Macky's formula applies to the sparking field for water drops falling in a vertical field and to the corona field for water drops falling in a horizontal field. Macky gave no information concerning temperature effects. Because of the possible importance of supercooled water drops in initiating lightning discharges and in consideration of charge generation mechanisms in thunderstorms, the effect of reduction of temperature of water drops in strong electric fields was studied.

To supercool the water drops, a refrigerator was constructed in the shape of a vertical cylinder. Calculation of the amount of supercooling was based upon drops of radius 0.050 cm. and smaller. Difficulties were encountered in attempting to produce and control these small drops, therefore, larger drops were used. The larger drops were not cooled as rapidly in their fall through the cold air in the refrigerator.

Ludlam's equation (1930), for the heat balance of a falling particle is,

$$H_1 + H_2 = 4 \pi \theta r^2 K T^3 + 2400 k \pi C r p^*$$

Where H_1 is the rate of heat loss due to radiation and conduction, H_2 is the rate of heat loss due to evaporation and convection, $\theta = \frac{3.2 + 0.59(Re)^{1/2}}{2 r}$, $K = (573 + 1.8 T_c) \times 10^{-7}$,

$$k = \frac{0.239 \times (273 + T_c)^2}{(281)^2} \times \frac{1013}{p}, \quad C = 1 + 0.229 (Re)^{\frac{1}{2}}$$

Here Re is the Reynolds number, T_c is the air temperature in degrees Centigrade, p is the pressure in millibars, T^* is the difference in temperature between the spherical surface and the surrounding air, r is the radius of the sphere, and k, the diffusion coefficient of water vapor into air. C is a coefficient due to the relative air speed, K is the coefficient of conductivity of heat of the air, and p^* is the difference in vapor density between the drop surface and the undisturbed flow. H_1 and H_2 are given in cal./sec., T^* is in degrees Kelvin, r is in centimeters, k is in cm.²/sec., p^* is in gm./cm.³, and K is in cal./cm.² -sec. -deg. C./cm.

Since the drops started with zero initial velocity, and approached some fraction of their terminal velocity, Ludlam's equation was integrated with respect to time.

Gunn & Kinzer (1949), assume that for drops larger than 0.0080 cm. diameter falling in air, the resistive force is proportional to the velocity of the drop squared. The following equation was written and solved for V as a function of t.

$$m \frac{dV}{dt} = mg - kV^2$$

V as a function of t is:

$$V = V_t \left(\frac{e^{2 (kg/m)^{\frac{1}{2}} t} - 1}{e^{2 (kg/m)^{\frac{1}{2}} t} + 1} \right)$$

Where $V_t = (mg/k)^{\frac{1}{2}}$ cm/sec., $g = 980$ cm/sec.², m = mass of the

drop in grams, and $k = mg/V_T^2$ gm/cm.

The equation for V was integrated with respect to time to get h , the distance the drop fell.

$$h = \frac{m}{k} \left[\ln (1 + e^2 (kg/m)^{\frac{1}{2}} t) - \ln 2 - (kg/m)^{\frac{1}{2}} t \right]$$

Since h was known (170 cm. during most observations), t was found by successive approximations. By knowing t and the other parameters in the equation for V for a given size drop, V was calculated. For the sizes of drops used in the experiments it was found that the drops were within 2% of their terminal velocity after a fall of 170 cm.

The Reynolds number is a function of drop size and velocity of fall. According to Gunn & Kinzer (1949), the Reynolds number is: $Re = \frac{2}{\mu} \rho r V$, where V is a function of time. The values of Re , θ , K , C , and k were substituted into Ludlam's equation. Ludlam's equation was integrated with respect to time, assuming r was a constant, to get the amount of heat transferred in calories:

$$\int_0^t (H_1 + H_2) dt = -2 \pi r T^* 10^{-7} \left[1834t + 5.8 T_c t + (338 + 1.06 T_c) \left(\frac{2r V_T m}{\mu K} \right)^{\frac{1}{2}} \left[\tanh^{-1} (\tanh \sqrt{kg/m} t)^{\frac{1}{2}} - \tanh^{-1} (\tanh \sqrt{kg/m} t)^{\frac{1}{2}} \right] - 23.1 r p^* \frac{T_K^2}{P} \left[t + 0.229 \left(\frac{2r V_T m}{\mu K} \right)^{\frac{1}{2}} \left[\tanh^{-1} (\tanh \sqrt{kg/m} t)^{\frac{1}{2}} - \tanh^{-1} (\tanh \sqrt{kg/m} t)^{\frac{1}{2}} \right] \right] \right]$$

Where μ_K is the kinematic viscosity of air at temperature T_K , in cm^2/sec .

This equation was solved to find the amount of heat lost from the drops examined. The temperature of the drops between the field plates, T_f , was calculated from:

$$m_f C_p T_f = m_0 C_p T_0 + \int_0^t (H_1 + H_2) dt$$

assuming that C_p , the specific heat capacity at constant pressure, was unity; and that the final mass of the drop, m_f , was the same as the initial mass, m_0 .

The mass lost by the drop was calculated from the second term on the right hand side of the equation. By dividing this term by 600 calories per gram, the mass lost is obtained. Calculations of the mass lost by the drops showed that it was negligible.

The calculated temperatures are given in Tables 1 and 2. These are expected to be the minimum amount of cooling for the drops because the humidity was assumed to be 100%. A calculation of the maximum amount of cooling showed that instead of 0.5 degrees Centigrade of cooling, twice this amount, or about 1.0 degree of cooling would be obtained if the humidity of the air was zero.

The parameters in Ludlam's equation were corrected for temperature and pressure whenever values of their variation were available.

Loeb and Meek (1941) showed that $E/P = \text{constant}$, where E is the breakdown electric field for air in volts per

centimeter, and P is the atmospheric pressure in millimeters of mercury, (except at extremely low pressures).

A calculation was made of $E/P = \text{constant}$ for the values of pressure given in the NACA standard atmosphere. Another calculation of $E = 447 (S/r)^{1/2}$ was made taking into account the variation of surface tension with temperature, for the NACA standard atmospheric temperatures. Estimated values for the surface tension of water were used below -8 degrees Centigrade.

The values of field calculated by these two methods (Table 7), indicate that near the 8 km. level in the atmosphere the pressure dependence of the corona and sparking fields begins to control the behaviour of water drops in strong electric fields instead of the surface tension dependence on temperature. However, since the temperature at the 8 km. level is about -37 degrees Centigrade, droplets with radii larger than 0.005 cm. are nucleated at that temperature, (Hoffer, 1961). Therefore within a thunderstorm cloud, surface tension effects control the distortion, disruption, corona onset, and sparking fields of water drops up to near the 8 km. level. However, temperatures within clouds will be higher than in the surrounding air. Hence, surface tension control of fields of water drops may be diminished in vigorous storms.

APPARATUS

Refrigerator

A refrigerator was constructed in the shape of a vertical cylinder two meters high. It was constructed in two sections fitted together by threaded ends. Seventy-five feet of 3/8 inch copper refrigeration tubing was attached in sections running lengthwise along an aluminum pipe of inside diameter 10 inches and 3/8 inch wall. This was used as the core of the refrigerator. Three observation ports, 32 inches long and 2 inches wide, were cut into each section at 90 degree intervals. The copper tubing was clamped tightly against the outside of the aluminum core by channel aluminum strips. A bakelite ring at each end of each section spaced the outside aluminum shell away from the copper coils. First a vermiculite insulation was used between the aluminum pipe and the outer shell. A leak developed inside the refrigerator and for the reassembled apparatus, styrofoam sheets were cut into strips and used as insulation. Thin stainless steel was fitted around each observation port to retain the insulation and give the outer aluminum shell rigidity. Styrofoam strips were cut and used as plugs for observation ports which were not being used.

The refrigerator was mounted vertically on a stand constructed from a steel plate 1/2 inch thick. Steel legs

at each corner with a 1/2 inch diameter bolt through a small plate on the bottom of each made leveling of the refrigerator possible.

The outside of the refrigerator was wrapped with glass wool insulation. A foil layer on the outside was used to reflect as much heat as possible. Styrofoam 2 inches thick and 10 inches in diameter was used to plug the lower end of the refrigerator. A small hole cut in the center of the styrofoam plug allowed water drops to fall through after examination in the electric field.

A Copeland Model K-33-C refrigeration compressor unit was used with freon 22 refrigerant. A photograph of the drop tower and compressor unit is shown in Figure 1.

Temperature Measurement

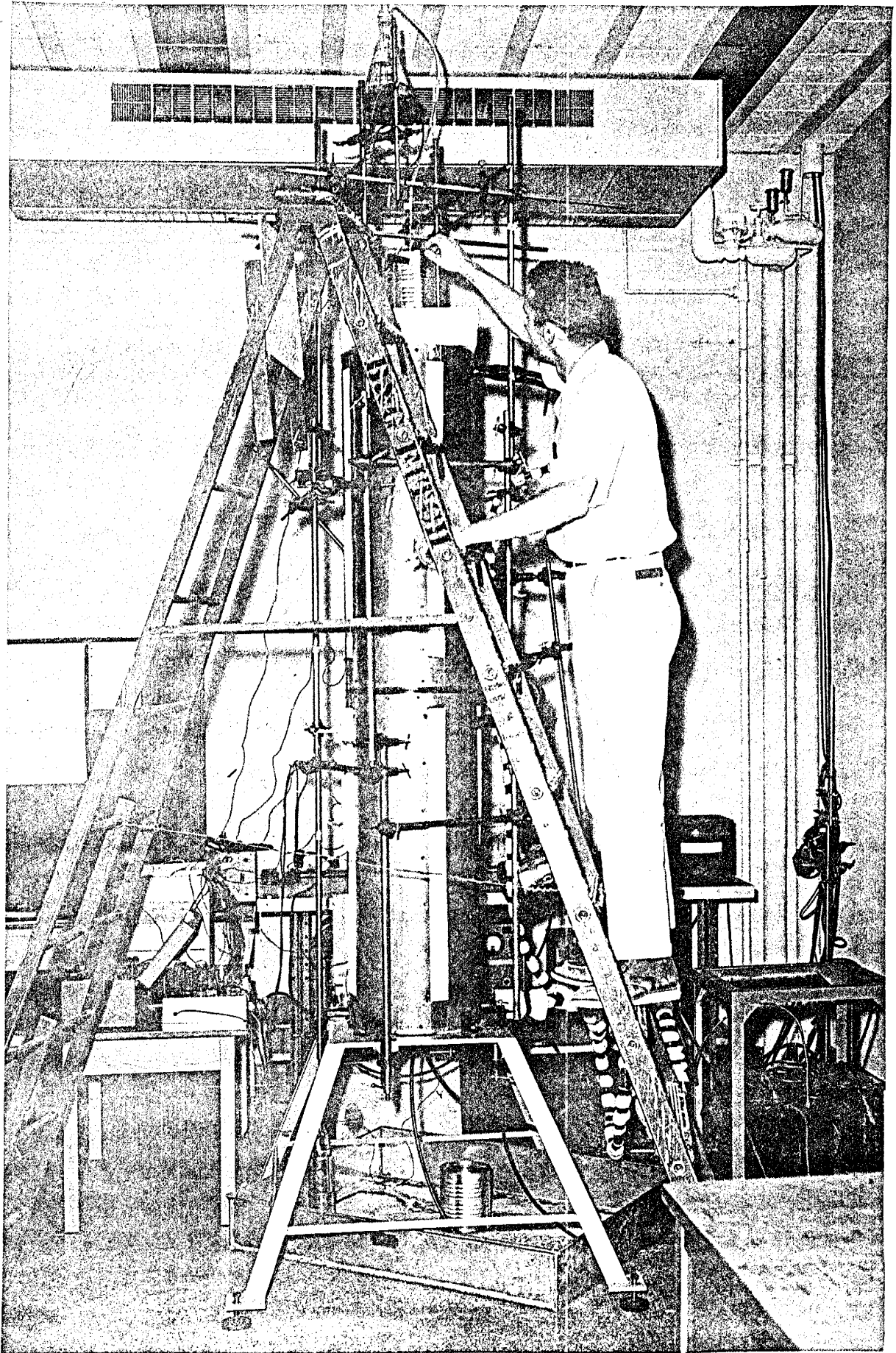
Temperature was measured by using glass thermometers and iron-constantan thermocouples. The reference junction was placed in ice water along with a glass thermometer. A Leeds-Northrup potentiometer (catalogue #8693) was used to measure the output difference in millivolts between the thermocouple and the reference junction.

The millivolt scale of the potentiometer was read to plus or minus 0.01 millivolt. The temperature was known to plus or minus 0.2 degrees Centigrade.

The glass thermometers were scaled in divisions of 0.2 degrees Centigrade from -50.0 to 50.0 degrees.

FIGURE 1

PHOTOGRAPH OF REFRIGERATED DROP TOWER



Temperatures observed include initial water temperature, room air temperature, refrigerator air temperature, and refrigerator wall temperature.

Water Droppers

Glass tubing drawn out into a narrow capillary tip was used as a water dropper. Several different sizes were made and used. It was found that different sizes of drops could be produced by varying the rate of water flow through the dropper. A 1,000 ml. Erlenmeyer flask was used as a reservoir for the distilled water. This was mounted at the top of the refrigerator and water was fed through plastic tubing by means of a siphon into a petcock. From the petcock, the water passed downwards through a glass tube to a coil of plastic tubing 6 feet long. This tubing was inside a can containing the cooling solution for precooling the water. The lower end of the plastic tubing was connected to a glass dropper. This dropper was fitted into a rubber stopper placed in a hole in the bottom of the cooling solution can.

The cooling solution container rested on a slab of styrofoam placed across the top of the refrigerator. A hole in the center of the styrofoam allowed adjustment of the position of the dropper so that the drops fell between the field plates.

The water dropper was calibrated at different dropping

rates by counting the number of drops necessary to fill a graduated cylinder to a certain volume. For example, at one drop per second, one dropper produced drops of radius 0.22 cm. The size of the drop was changed during many of the later runs. Drop size was measured at the end of each run before the petcock was shut off. The maximum spread in the measurements of a given drop radius was observed to be plus or minus 0.005 cm. Drop radii were rounded off to the nearest 0.01 cm.

Precooling Bath

To be certain that the water drops being examined at cold temperatures were as cold as possible before dropping, a precooling bath was constructed. A coil of approximately 6 feet of plastic tubing was placed inside a large tin can. Water from the reservoir passed through the coil very slowly as the water drops fell from the dropper. Ice and water placed in the can completely covered the coil of plastic tubing. Salt (NaCl) and magnesium chloride (MgCl_2) were used separately to lower the melting point temperature of the ice. With sodium chloride, the melting point of the ice was lowered about 3.5 degrees Centigrade. With magnesium chloride, the melting point of the ice was lowered about 5.0 degrees Centigrade. The temperature of the precooling bath was monitored with a thermocouple. The temperature at which the water drops left the dropper was assumed to be the same as that of the precooling bath.

The three final runs were made using methanol in the precooling bath. The methanol was refrigerated in a freezer until its temperature was near -10 degrees Centigrade. An attempted run at -15 degrees Centigrade resulted in the freezing of the water inside of the dropper and precooling coil.

Field Plates and Electric Field

Field plates were made from aluminum bar stock 3 inches wide, 12 inches long, and 3/8 inch thick. The edges were rounded and polished. The front and back of each plate was also polished smooth.

The field plates were mounted vertically on lucite angles by means of nylon screws. The lucite angles rode on a flat piece of lucite between two rails and were adjustable for any plate spacing up to 2 1/4 inches. The entire field plate assembly, including the lucite base, could be placed at any height within the refrigerator pipe and held there by setscrews.

A clamp to hold the plates parallel was made from two lucite bars and two nylon screws. This clamp was made after observing that the separation of the field plates was greater at the top than at the bottom. When this difference in separation was observed, results of observations were not in agreement with Macky's results. After the clamp was installed, the observations agreed very well with those of Macky. The error in measuring

the spacing of the field plates was estimated to be not more than 5%.

A Beta Electronics, 0 to 30 kilovolt, power supply was connected to the field plates. One field plate was connected to ground. A Sensitive Research electrostatic voltmeter was connected between the 0 to 30 kilovolt power supply and ground. Potential differences applied to the plates were read from the electrostatic voltmeter. The potential difference was divided by the plate spacing to obtain the applied electric field.

Corona and Spark Detectors

1. The Eye

In a darkened room, a faint glow was visible to the eye as a drop passed through the field and emitted corona. Sparks were visible when the field was equal to or exceeded the critical sparking field.

2. The Ear

A hissing noise was heard from each drop as it passed through the field and emitted corona. A loud "zap" was heard each time a drop passed between the plates and sparking occurred.

3. Radio Receiver

The electromagnetic radiation emitted from corona and spark discharges was detected by placing the antenna of a short wave radio receiver near the field plates. As each drop emitting corona passed through the field, a burst

of static was audible on the radio loudspeaker. Sparks made a much louder static burst and were also audible.

4. Photographs

Photographs showed the corona emitted from the drops in the corona field. Sparks also were visible in the photographs of drops in critical and higher sparking fields. The onset of corona from photographs could not be determined as accurately as with the radio receiver.

Photography

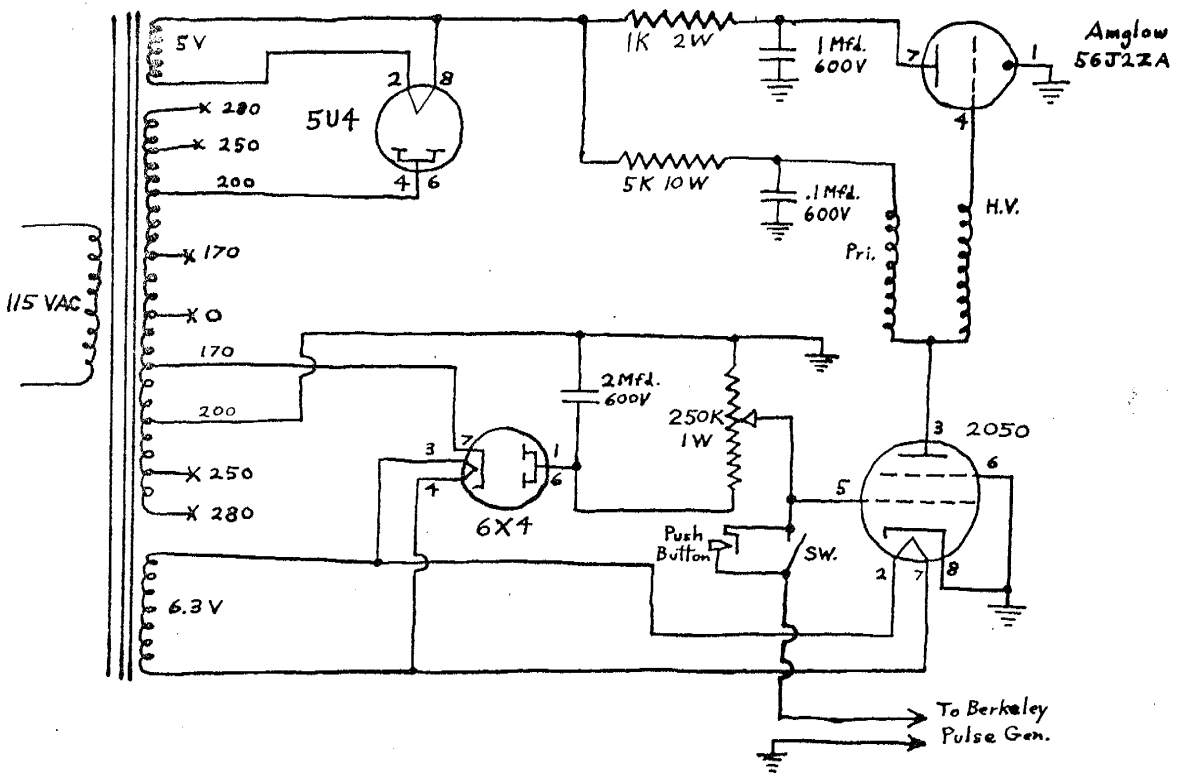
A Mitchell 35 millimeter movie camera, operated manually, was used with Tri-X film to photograph the falling drops. A 2 inch focal length lens with an aperture of f 2.8 was used. The subject distance was about 8 inches. A hand crank was used to advance the film after each exposure.

Illumination was achieved by using an Anglow 56J2Z-A flash tube in a stroboscopic circuit. The rate of flashing was variable from about one flash per second to about 100 flashes per second. This flashing rate was controlled by a Berkeley Double Pulse Generator connected to the grid of a 2050 thyatron. (Figure 2, Circuit Diagram)

The water dropper petcock was adjusted to give a water dropping rate of about one drop per second. A microswitch in the strobe circuit allowed flashing to be initiated at will. The flash tube was mounted behind a thin white paper background. With the flashing rate of the pulse generator set on 100 flashes per second, and

FIGURE 2

FLASH CIRCUIT



by use of the microswitch, one or two flashes were obtained as a drop passed through the field of view. About 25% of the photographs made showed drops.

Drops falling between the field plates were photographed under five general conditions:

1. With no field between the plates.
2. With low field between the plates.
3. With corona field.
4. With critical sparking field.
5. With a higher field than the critical sparking field.

Considerable difficulty was encountered in attempting to photograph the falling drops with front illumination. The intensity of the flash was not enough to expose the image of a drop. The simplest lighting method seemed to be illumination of the white paper background from behind but difficulty was encountered from multiple flashing which reduced the contrast. Nevertheless, photographs of drops were obtained. (Figure 3.)

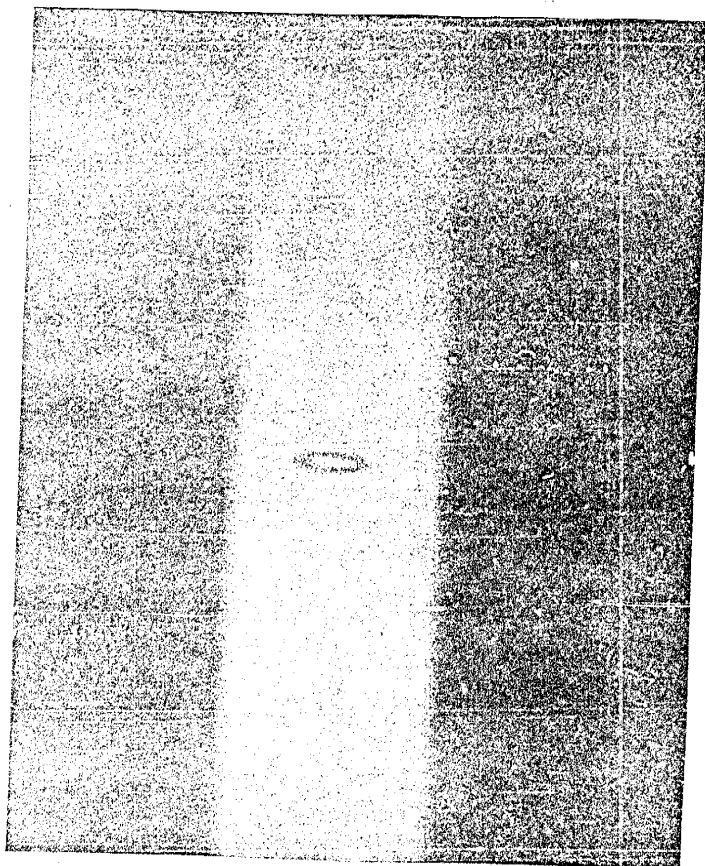
Pressure Measurement

A Tycos compensated dial type barometer was used for observations of atmospheric pressure. Barometer readings were not reduced to sea level. The dial of the barometer is calibrated in graduations of 0.1 cm. of mercury from 64.0 cm. Hg. to 79.0 cm. Hg. Interpolation between the 0.1 cm. Hg. divisions allowed reading of the barometer to plus or minus 0.02 cm. of Hg.

The barometer was calibrated and set by use of a

FIGURE 3

PHOTOGRAPH OF A WATER DROP IN ITS CORONA FIELD



This photograph is of a 0.21 cm. radius water drop in its corona field of 8,700 volts per cm. The distortion ratio, which is the ratio of the horizontal to the vertical dimension of the drop, is $D_h/D_v = 3.75$. The field plate spacing is 2 cm, and temperature of the drop is 27 degrees Centigrade. The positive field plate is on the right. The drop is elongated in the direction of the field. In the lower part of the picture, the path of the falling drop is outlined by corona. The light spot in the drop is forward scatter of the light from the white background. This photograph is #11-4, Run 14.

precision mercury barometer. Periodic checks were made between the Tyco's barometer and the mercury barometer. Pressure was recorded during each run. From the work of Loeb and Meek (1941) and Table 7, it can be seen that a pressure change does not affect the results until the pressure has been reduced to about 240 mm. Hg. The observed pressure during the observations was around 650 mm. Hg.

OBSERVATIONS

Barometric pressure, room temperature, refrigerator air temperature, refrigerator wall temperature, initial water temperature, approximate drop fall height, plate spacing, corona potential, sparking potential, and drop radius were recorded during each run.

A summary of the primary observations from each run appears in Table 1.

Another tabulation of drop temperature, corona field, and spark field arranged in order of increasing drop radius, is given in Table 2. Table 2 shows that there is an increase in the corona and sparking fields with a decrease in drop radius.

Table 3, the difference in percent between the highest and lowest values of the fields at constant temperature, illustrates that the average deviation of the observed field for a given drop size is about 2%.

A graph, Figure 4, of corona field vs. drop temperature was made from the data in Table 2. A distinct increase of corona field with a decrease in temperature is shown, especially in the results of 0.15 cm. radius drops. For the drops labeled N, there is a large spread in the measurements just below 0 degrees Centigrade. The highest values of the corona field are favored because difficulty was encountered in the cleaning of the water, ice, and frost from the field

27

FIGURE 4

CORONA FIELD (kv/cm) VS. DROP TEMPERATURE (°C)

Key for Figure 4

L -- 0.13 ± 0.005 cm radius drops
M -- 0.14 ± 0.005 cm radius drops
N -- 0.15 ± 0.005 cm radius drops
O -- 0.18 ± 0.005 cm radius drops
S -- 0.21 ± 0.005 cm radius drops
U -- 0.22 ± 0.005 cm radius drops

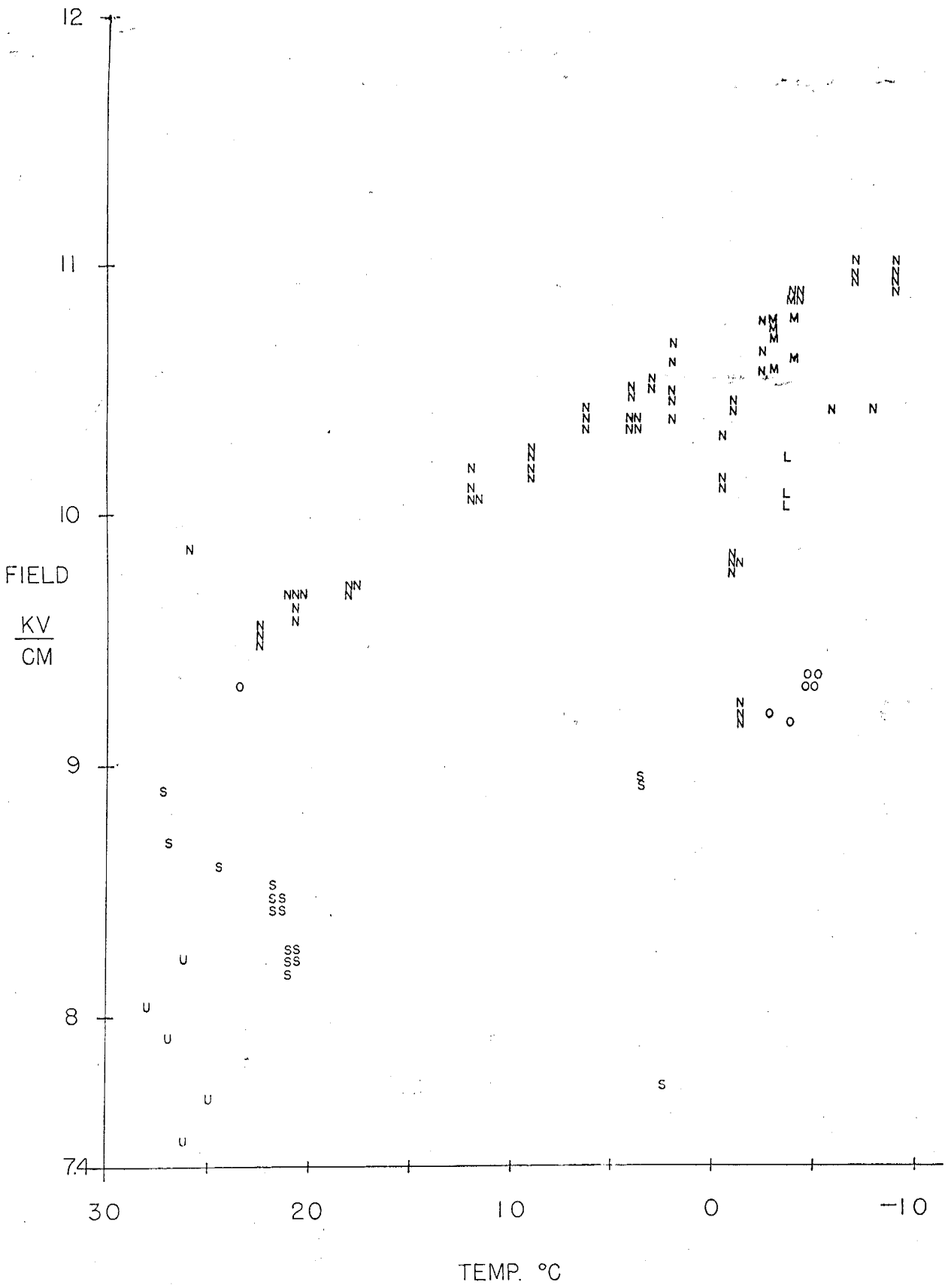


FIGURE 4

plates. It was also observed that as successive observations were made of the corona and sparking fields, without attempting to clean the plates, a decrease in these fields occurred. The corona discharge may have taken place at the wet field plates and may not have come from drop disruption.

An empirical equation for the corona field was written for the data of 0.15 cm. radius drops in Figure 4. Macky's equation was used as a basis for the empirical equation which is;

$$E = 447 \frac{(S_0 + a + bT + cT^2)^{\frac{1}{2}}}{(r)^{\frac{1}{2}}}$$

$S_0 = 75.6$ dynes per cm., the surface tension of water at zero degrees Centigrade, $a = 8.8$, $b = -.77$, and $c = 0.0039$. Using the following values of field the constants a , b , and c were calculated.

$$E = 11,000 \text{ v/cm. at } -8 \text{ degrees C.}$$

$$E = 10,600 \text{ v/cm. at } 0 \text{ degrees C.}$$

$$E = 9,700 \text{ v/cm. at } +20 \text{ degrees C.}$$

The observations agree with the empirical equation within a few percent except for those low values below zero degrees Centigrade which are assumed to be diminished from the true value because of ice and frost growth on the field plates.

The corona field of the 0.15 cm. radius drops increases about 13% from around 9,700 volts per cm. at +20 degrees Centigrade to around 11,000 volts per cm. at -8 degrees Centigrade.

A graph, Figure 5, of sparking field vs. temperature

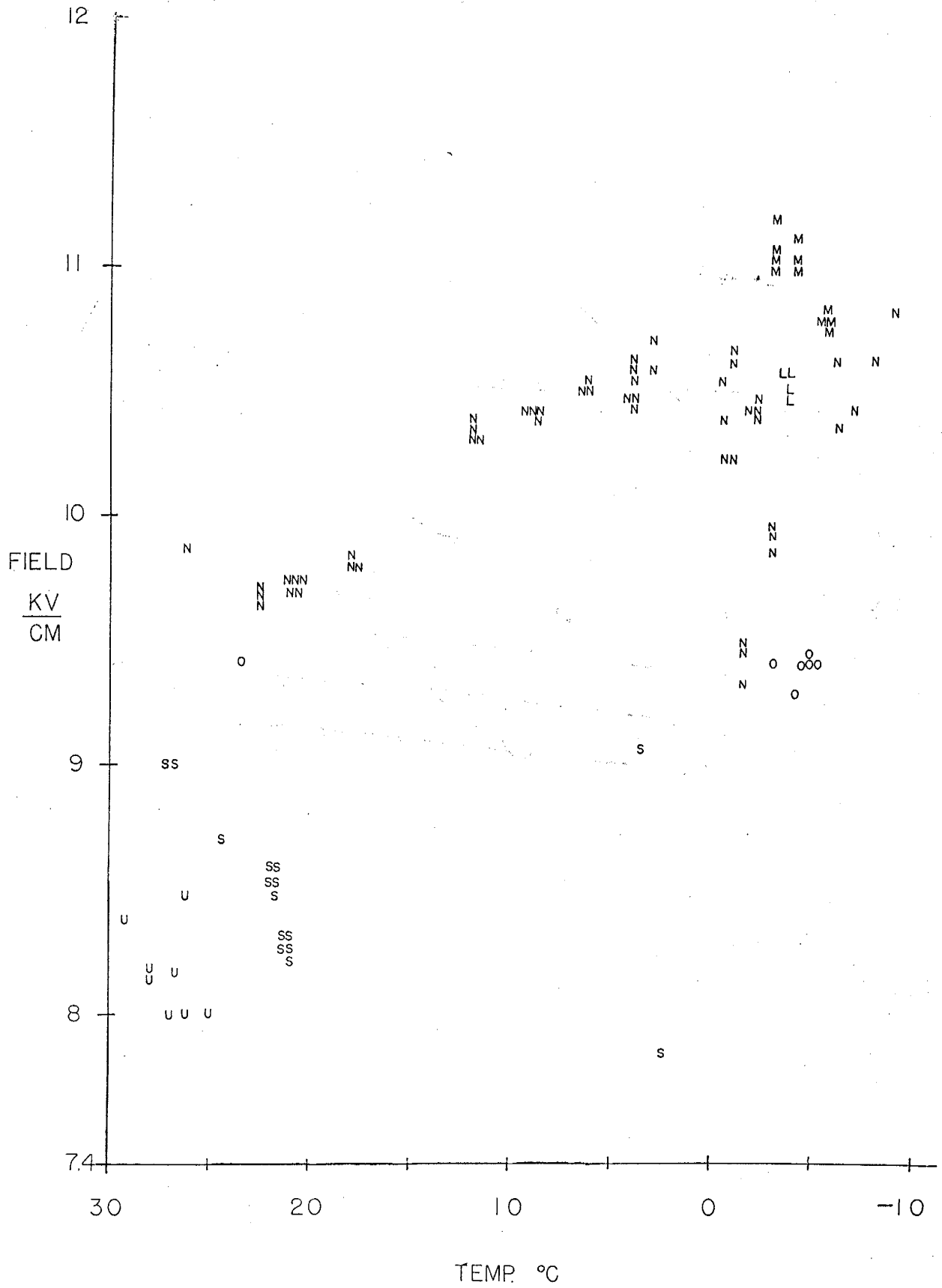
FIGURE 5

SPARKING FIELD (kv/cm) VS. DROP TEMPERATURE (°C)

Key for Figure 5

L -- 0.13 ± 0.005 cm radius drops
M -- 0.14 ± 0.005 cm radius drops
N -- 0.15 ± 0.005 cm radius drops
O -- 0.18 ± 0.005 cm radius drops
S -- 0.21 ± 0.005 cm radius drops
U -- 0.22 ± 0.005 cm radius drops

FIGURE 5

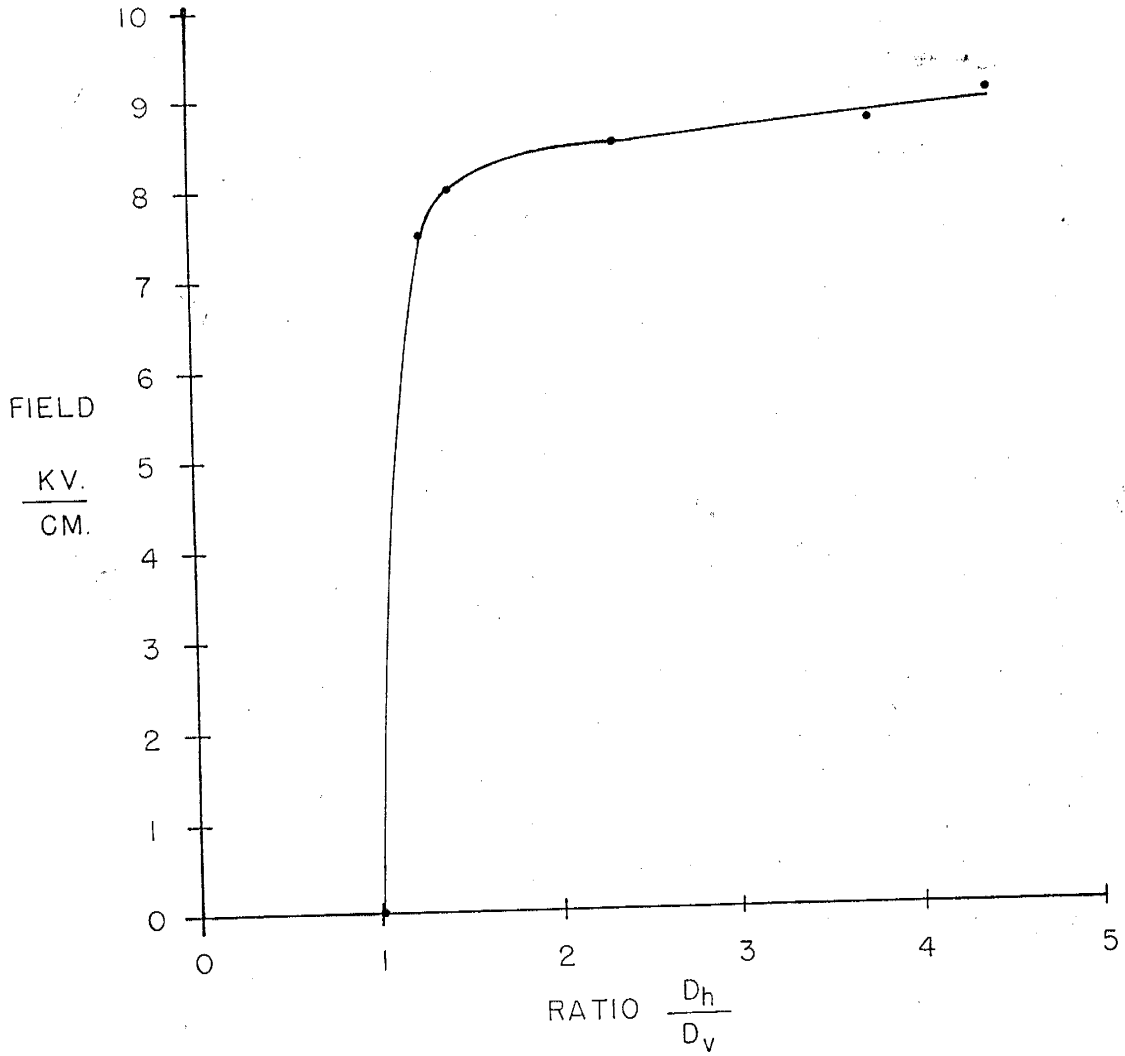


was made from the data in Table 4. This graph illustrates that as the temperature decreases the sparking field for a given size drop increases. The sparking field measurements may not be too accurate because of the possibility of applying a greater potential difference to the field plates than the critical sparking value. Also, the close field plate spacing may have had an effect in causing breakdown.

Figure 6, field in kv/cm vs. ratio (D_h/D_v) was made from measurements of photographs of drop distortion, Table 4. D_h is the horizontal length of the drop in the direction of the field. D_v is the vertical drop length perpendicular to the field. The ratio D_h/D_v is the horizontal length of the drop divided by the vertical length of the drop. Figure 6 shows that a drop of 0.21 cm. radius is not distorted much by an increase in field up to around 7,500 volts per cm, where the distortion ratio is 1.25. With further increase in the field to 8,700 volts per cm. (at which value corona occurred), the ratio increases rapidly to 3.75. Sparking occurred at 9,600 volts per cm. at a ratio D_h/D_v of 4.40. The drop distortion data may be valuable for polarization calculations in radar experiments.

FIGURE 6

FIELD VS. DISTORTION RATIO



DROP RADIUS = 0.21 cm.

SUMMARY AND CONCLUSIONS

The author constructed a refrigerator in the form of a vertical cylinder. Water drops were dropped through the refrigerated air and between two polished aluminum field plates supported by a lucite framework. The water drops were precooled to near zero degrees Centigrade in order that supercooling might be achieved more easily within the limited fall distance. Ludlam's equation (1950), was used to calculate the amount of supercooling that would be achieved by water drops of different size falling through air at temperatures below zero degrees Centigrade. The sparking and corona fields for different drop sizes at different temperatures were observed. At water temperatures below zero degrees Centigrade, a great amount of difficulty was encountered due to the freezing of water on the field plates resulting from the breakup of the drops during application of the field.

A study was made of the corona and sparking fields for freely falling water drops ranging in radius from 0.13 cm. to 0.22 cm. at temperatures ranging from -9 degrees Centigrade to 29.2 degrees Centigrade. It was observed that the corona and sparking fields of water drops in air increase with a decrease in temperature. The increase in corona and sparking fields cannot be ascribed to an error in measuring the drop size. The 13% increase in corona and

sparkling fields with a decrease in temperature for a given size of drop is ascribed partly to a surface tension increase with temperature decrease and partly to reasons unknown at this time.

Distortion of the drops increases gradually with an increase in field until about 85% of the sparking field value is reached. The last 15% increase in the field, to the sparking value, increases the distortion of the drop from a ratio of 1.25 to 4.40.

The theoretical value of the applied field which should cause disruption and corona, $E_0 = 2240 (S/r)^{1/2}$, is not a good approximation for water drops in strong electric fields. It must be remembered that this equation was derived for a spherical drop in a uniform field. The photographs of drops in strong electric fields show that the drops appear elongated in the direction of the field.

Since the curvature is greatest at the ends of the drop in the direction of the field, the field is more concentrated at these ends than was expected for a spherical drop of the same volume as the elongated one. Therefore, the higher field at the ends of the drop causes disruption and corona emission to occur before the applied field reaches the theoretical value. In fact, the drop breakup field was nearly the same as predicted from Macky's equation, $E_0 = 447 (S/r)^{1/2}$.

Supercooled water drops require higher values of

electric field to cause corona and spark discharges than that required by water drops at room temperature.

The pressure dependence of the breakdown electric field for air is not expected to have any effect upon water drops in thunderstorm clouds below the 8 km. level.

An empirical equation for the observed corona field is:

$$E = 447 \frac{(75.6 + 8.8 - 0.77T + 0.0039 T^2)^{\frac{1}{2}}}{(r)^{\frac{1}{2}}}$$

This formula takes the drop temperature into consideration.

SUGGESTIONS FOR FURTHER INVESTIGATION

More information is needed about the corona and sparking fields of supercooled water drops. The temperature should be decreased to study possible nucleation effects of the electric field on supercooled water drops. If the drop size is reduced, more supercooling of the water could be achieved.

The distortion ratio of water drops should be studied as a function of drop size and temperature. This information should be valuable in polarization studies of thunderstorms by radar.

The dependence of drag coefficient on drop size and speed should be examined.

A careful investigation of the effect of contaminants on water drops in strong electric fields should be made.

Pressure simulation of natural thunderstorm conditions in the laboratory and its effect on the corona and sparking fields of supercooled water drops in strong electric fields should be examined. Studies under actual pressure conditions as exist within thunderstorm clouds merit further investigation.

APPENDIX

37
TABLE 1

SUMMARY OF PRIMARY OBSERVATIONS FROM EACH RUN

Run No.	Radius (cm)	Drop Temp. (deg C)	Barometer (mm.Hg)	E Spark (V/cm)	E Corona (V/cm)
1	0.22	29.2	656.0	---	---
2	0.22	29.2	656.0	8,380	---
3	0.22	26.2	658.7	8,480	8,240
4	0.22	28.0	657.5	8,140	---
5	0.22	28.0	657.5	8,190	8,040
6	0.22	27.0	656.2	8,000	7,920
7	0.22	27.6	654.0	---	---
8	0.22	25.0	651.8	8,000	7,670
9	0.22	28.2	650.0	---	---
10	0.22	26.7	647.2	8,170	---
11	0.15	26.4	---	---	---
11a	0.15	26.2	649.8	10,000	9,880
11b	0.22	26.2	649.8	8,000	7,500
12	0.21	---	---	---	---
13	0.21	24.5	653.0	8,700	8,600
14	0.21	27.0	652.2	9,000	8,700
15	0.21	27.3	654.4	9,000	8,990
17a	0.21	21.7	648.7	8,540	8,470
17b	0.21	21.0	648.7	8,280	8,230
17c	0.15	20.8	648.9	9,720	9,660
20	0.21	2.4	652.0	7,840	7,730
21	0.21	24.0	649.7	---	---

TABLE I
(continued)

Run No.	Radius (cm)	Drop Temp. (deg C)	Barometer (mm.Hg)	E Spark (V/cm)	E Corona (V/cm)
22	0.21	3.3	651.2	9,070	8,945
23	0.15	-1.5	---	9,420	9,210
24	0.15	-1.0	642.8	---	---
25	0.15	-1.0	---	10,620	10,440
25b	0.15	-1.1	647.5	10,230	9,830
26	0.18	23.6	652.7	9,410	9,320
26	0.18	-2.7	652.7	9,410	9,210
26	0.18	-4.0	652.7	9,290	9,180
27	0.18	-4.4	649.5	9,420	9,350
28	0.13	-3.6	644.7	10,530	10,120
29	0.14	-5.3	651.2	10,790	---
30	0.15	-2.3	652.2	10,430	---
31	0.14	-3.8	642.2	11,040	10,760
32	0.14	-2.7	642.2	11,060	10,710
33	0.15	-4.1	648.8	10,830	---
33	0.15	-8.7	648.8	10,630	10,430
33	0.15	-7.2	648.8	10,430	---
33	0.15	-6.4	648.8	10,360	---
33	0.15	-6.2	648.8	10,630	10,430
34	0.15	-9.0	646.0	---	10,960
34	0.15	-7.0	646.0	---	10,980
34	0.15	-4.1	646.0	---	10,890
34	0.15	-2.7	646.0	---	10,670

TABLE 1
(continued)

Run No.	Radius (cm)	Drop Temp. (deg C)	Barometer (mm.Hg)	E Spark (V/cm)	E Corona (V/cm)
34	0.15	1.9	646.0	---	10,530
34	0.15	2.9	646.0	10,550	10,530
34	0.15	3.9	646.0	10,520	10,410
34	0.15	6.3	646.0	10,520	10,390
34	0.15	8.9	646.0	10,420	10,210
34	0.15	11.9	646.0	10,340	10,110
35	0.15	-3.0	648.4	9,910	9,800
35	0.15	-0.4	648.4	10,390	10,190
35	0.15	17.4	648.4	9,810	9,710
35	0.15	22.5	648.4	9,680	9,530

TABLE 2

DROP TEMPERATURE, CORONA FIELD, AND SPARK FIELD

Arranged in order of increasing drop radius

Radius (cm)	Drop Temp. (C)	Corona Field (v/cm)	Spark Field (v/cm)		
0.13	-3.6	10,090	10,470		
		10,040	10,590		
		---	10,520		
		10,230	10,590		
0.14	-2.7	10,710	10,980		
		10,790	11,180		
		10,750	11,020		
		10,590	11,060		
	-3.8	10,790	10,980		
		10,870	11,020		
		10,630	11,110		
	-5.3	---	10,790		
		---	10,750		
		---	10,830		
		---	10,790		
		0.15	-9.1	---	10,830
				10,430	10,630
-8.2	---		10,430		
	---		10,360		
-7.2	10,430		10,630		
	9,580		9,690		
-6.4	9,690	9,740			
	9,630	9,690			
-6.2	9,690	9,740			
	9,690	9,740			
20.8	10,420	10,670			
	10,460	10,620			
-1.0	9,830	10,230			
	9,250	9,450			
	9,210	9,490			
-1.5	9,170	9,330			
	---	10,430			
-2.3	---	10,430			
	---	10,400			
	---	10,470			
	22.5	9,530	9,720		
	9,560	9,680			
	9,490	9,650			

TABLE 2
(continued)

Radius (cm)	Drop Temp. (°C)	Corona Field (V/cm)	Spark Field (V/cm)
0.15	-9.0	10,970	---
		11,020	---
		10,900	---
		10,940	---
	-7.0	11,020	---
		10,940	---
		10,970	---
		10,900	---
	-4.1	10,860	---
		10,900	---
		10,900	---
		10,580	---
	-2.7	10,780	---
		10,660	---
		9,810	9,920
		9,770	9,960
		9,810	9,850
		10,320	10,550
		10,150	10,390
		10,110	10,290
1.9		10,620	---
		10,700	---
	10,500	---	
	10,390	---	
	10,460	---	
2.9	10,520	10,590	
	10,550	10,710	
3.9	10,390	10,550	
	10,470	10,590	
	10,510	10,630	
	10,350	10,470	
	10,390	10,430	
	10,350	10,470	
	10,390	10,550	
	10,350	10,510	
6.3	10,430	10,510	
	10,190	10,430	
	10,270	10,390	
	10,240	10,430	
11.9	10,150	10,430	
	10,070	10,350	
	10,110	10,310	
	10,070	10,390	
	10,190	10,310	
17.4	9,720	9,800	
	9,680	9,800	
	9,720	9,840	
	9,870	10,000	
26.2			

TABLE 2
(continued)

Radius (cm)	Drop Temp. (C)	Corona Field (V/cm)	Spark Field (V/cm)
0.18	23.6	9,320	9,410
	-2.7	9,210	9,410
	-4.0	9,180	9,290
	-4.4	9,320	9,410
		9,370	9,410
		9,320	9,410
		9,370	9,450
0.21	24.5	8,600	8,700
	27.0	8,700	9,000
	27.2	8,900	9,000
	21.7	8,480	8,590
		8,530	8,590
		8,480	8,530
		8,430	8,530
		8,430	8,480
	2.4	7,730	7,840
	3.3	8,960	9,070
		8,930	---
	21.0	8,170	8,220
		8,270	8,320
		8,270	8,320
		8,220	8,270
		8,220	8,270
0.22	29.2	---	8,380
	25.2	8,240	8,480
	28.0	---	8,140
		8,040	8,190
	27.0	7,920	8,000
	25.0	7,670	8,000
	26.7	---	8,170
	26.2	7,500	8,000

--- indicates not sufficient data to compute

TABLE 3

PERCENT DIFFERENCE BETWEEN THE HIGHEST AND LOWEST VALUES OF THE FIELD AT CONSTANT TEMPERATURE

Radius (cm)	Temp. (°C)	Corona Field (%)	Spark Field (%)
0.13	-3.6	2	1
0.14	-2.7	2	2
	-3.8	2	1
	-5.3	--	1
0.15	-9.1, -8.2	--	2
	-8.2, -7.2	--	2
	-7.2, -6.4	--	1
	-6.4, -5.2	--	3
	20.8	1	1
	-1.0	6	4
	-1.5	1	2
-2.3	--	1	
0.18	-4.4	1	1
0.21	27.0, 24.5	1	3
	21.7	1	1
	21.0	1	1
0.22	29.2, 28.0	--	3
	28.0	--	1
	27.0, 26.7	--	2
		2% average	2% average

-- indicates not sufficient data to compute

TABLE 4

DISTORTION OF 0.21 CM. RADIUS DROP

(taken from Run 14 photographs)

Field plate spacing --- 2.0 cm.
 Photograph field plate spacing --- 1.8 cm.
 Temperature --- 27.0 degrees C.

Photo No.	D_h cm	D_v cm	Ratio D_h/D_v	Applied Field (v/cm)
4-3				
4-9	.40	.40	1.00	0
9-10				
7-12				
7-15	.45	.36	1.25	7,500
8-4	.48	.33	1.46	8,000
8-10				
13-16	.67	.29	2.31	8,500
11-4				
12-13	.95	.25	3.75	8,700
12-14				
9-1	1.05	.24	4.40	9,000

D_h -- length of drop in the direction of field, i.e., horizontal

D_v -- length of drop in the direction perpendicular to field, i.e., vertical

Spark Field observed -- 9,000 volts per cm.

Corona Field observed -- 8,700 volts per cm.

RESULTS OF CALORIMETER CHECK OF LUDLAM'S EQUATION

Ludlam's equation (1950), gives 23.8 degrees C. as the final temperature of a drop of radius 0.15 cm, falling 2 meters through the air at -20.0 degrees C. when the initial temperature of the drop is 26.2 degrees C.

Conditions During Calorimeter Check

Refrigerator air temperature	-20.0 deg. C.
Initial water temperature	26.2 deg. C.
Initial room temperature	21.0 deg. C.
Empty calorimeter mass	208.20 gm.
Calorimeter plus water mass	209.90 gm.
Calorimeter plus water plus 50 drops of water mass	210.56 gm.
Initial mass of water in calorimeter	1.70 gm.
Mass of 50 drops of water added (by weight)	0.66 gm.
Mass of 50 drops of water calculated from observed radius of 0.15 cm.	0.68 gm.
Initial water temperature in calorimeter	19.4 deg. C.
Final water temperature in calorimeter	20.6 deg. C.
Final drop temperature (by weight method)	23.6 deg. C.
Final drop temperature (by calculated weight method)	23.5 deg. C.

CALCULATION OF EXPECTED ERROR IN DROP RADIUS

$$V = \frac{4}{3} \pi r^3 N D$$

Volume = V

Radius = r

Number of drops = N = 100

Density of water = D = 1.00

$$4.4 \text{ cc.} = 4.19 r^3 100 1.00$$

$$r = 0.22 \text{ cm.}$$

Error in reading graduated cylinder (plus or minus 0.1cc.)

$$4.3 \text{ cc.} = 4.19 r^3 100 1.00$$

$$r = 0.218 \text{ cm.}$$

$$4.5 \text{ cc.} = 4.19 r^3 100 1.00$$

$$r = 0.222 \text{ cm.}$$

$$\text{Error} = \frac{.002 \text{ cm.} \times 100\%}{.220 \text{ cm.}} = +1\%$$

TABLE 6

EXPECTED ERRORS OF MEASUREMENTS

Drop Radius	-----	± 1. %
Temperature	-----	± 0.2 °C.
Surface Tension	-----	± 0.2 %
Pressure	-----	± 0.03%
Drop Fall Height	-----	± 0.5 %
Voltage (V)	-----	± 0.5 %
Plate Spacing	-----	± 5. %
Corona Field	-----	± 6. %
Spark Field	-----	± 6. %

TABLE 7

VALUES OF FIELD CALCULATED FROM NACA STANDARD ATMOSPHERE
PRESSURES AND TEMPERATURES

Altitude (km)	Temp. (°C)	Pressure (mm Hg)	$E=39.5 P$ (v/cm)	$E=447 (S/r)^{1/2}$ (v/cm)	Surface Tension (dynes/cm)
0	15	760	30,000	8,570	73.5
2	2	596	23,600	8,600	75.4
3.5*	-8	--	--	8,780	77.0
4	-11	462	18,300	---	--
5.3*	-20	--	--	8,940	80*
6	-24	354	14,400	---	--
8	-37	267	10,600	9,120	83*
10	-50	198	7,820	9,220	85*
12	-55	145	5,730	---	--
14	-55	106	4,190	---	--

$r = 0.20$ cm.

* Indicates estimated value.

BIBLIOGRAPHY

- Barnard, V., The Approximate Mean Height of the Thundercloud Charges Taking Part in a Flash to Ground, Jour. Geophys. Res., v. 56, 1951, p.33-35.
- Best, A. C., The Size of Cloud Droplets in Layer Type Clouds, Quart. Jour. Roy. Met. Soc., v. 77, 1951, p.241-248.
- Bigg, E. K., The Supercooling of Water, Proc. Phys. Soc., v. 66B, 1953, p.688-694.
- Byers, Horace R., Thunderstorms, Compendium of Meteorology, Am. Met. Soc., U. of Chicago, Waverly Press Inc., Baltimore, Md., U.S.A., 1951, p.681-693.
- Dorsey, N. E., Properties of Ordinary Water Substance, Am. Chem. Soc., Rheinhold Pub. Corp., New York, U.S.A., 1940, p.375, p.514.
- Dorsch, R. G., and P. T. Hacker, "Photomicrographic Investigation of Spontaneous Freezing Temperatures of Supercooled Water Droplets", NACA Tech. Note 2142, Washington, July 1950, p.1-57.
- _____, and Joseph Levine, "A Photographic Study of Freezing of Water Droplets Falling Freely in Air", NACA RME 51L17, Feb. 25, 1952, p.1-29.
- English, W. N., Corona From a Water Drop, Phys Rev., v. 74, July 15, 1948, p.179-189.
- Frith, R., The Size of Cloud Particles in Stratocumulus Cloud, Quart. Jour. Roy. Met. Soc., v. 77, 1951, p.441-444.
- Gunn, Ross, The Electrical Charges on Precipitation at Various Altitudes and its Relation to Thunderstorms, Phys. Rev., v. 71, 1947, p.181-186.
- _____, Electric Field Intensity Inside of Natural Clouds, Jour. App. Phys., v. 19, 1948, p.481-484.
- _____, Electronic Apparatus for the Determination of the Physical Properties of Freely Falling Raindrops, Rev. Sci. Instr., v. 20, 1949, p.291-296.
- _____, The Hyperelectrification of Raindrops by Atmospheric Electric Fields, Jour. Met., v. 13, 1956, p.283-288.

_____, AND G. D. Kinzer, The Terminal Velocity of Fall for Water Drops in Stagnant Air, Jour. Met., v. 6, 1949, p.243-248, Table 2, p.246.

Handbook of Chemistry and Physics, 31st Ed., 1949, The Chemical Rubber Pub. Co., Cleveland, Ohio, U.S.A., p.1728, 1747, 1721, 1791.

Handbook of Chemistry and Physics, 42nd Ed., 1960-61 The Chemical Rubber Pub. Co., Cleveland, Ohio, U.S.A., p.2260, 2440, 2448-2449, 2486.

Hardy, J. K., "Evaporation of Drops of Liquid", Reps. Mem. #2805, TAE Dept. Mech. Eng. 1, March 1947.

Heverly, J. Ross, Supercooling and Crystallization, Trans. Am. Geoph. Union, v. 30 N.2, 1949, p.205-210.

Hoffer, T. E., A Laboratory Investigation of Droplet Freezing, Jour. Met., v. 18, 1961, p.767, Fig.1.

International Critical Tables, 1st Ed., McGraw-Hill Book Co., Inc., New York, v. 5, 1929, p.2,62,213.

Johnson, J. C., Measurement of the Surface Temperature of Evaporating Water Drops, Jour. App. Phys., v.21, 1950, p.22-23.

_____, Physical Meteorology, The Tech. Press of the MIT AND John Wiley & Sons, Inc., New York, Chapman & Hall Ltd., London, 1954, Table 7.3, p.219, Fig.8.4, p.242, p.262-263, 301,386.

Kinzer, G. D., and R. Gunn, The Evaporation, Temperature, and Thermal Relaxation-Time of Freely Falling Water Drops, Jour. Met., v. 8, N.2, 1951, p.71-83.

Lapple, C. E., Particle Dynamics, Eng. Res. Lab., E. I. DuPont de Nemours & Co., Inc., March 1948, Table 1 and Exhibit L, Fig.1.

Levine, Joseph, "Statistical Explanation of Spontaneous Freezing of Water Droplets", NACA Tech. Note 2234, Dec. 1950, p.2-27.

Loeb, L. B., Thunderstorm Electricity, Experimental Contributions To The Knowledge of Charge Generation, U.of Chicago Press, Edited by H. R. Byers, 1953, p.160-161.

_____, and J. M. Meek, The Mechanism of the Electric Spark, Stan. Univ. Press, 1941, p.116-117.

_____, Static Electrification, Springer-Verlag, Berlin, Göttingen, Heidelberg, 1958, p.204-210.

Ludlam, F. H., The Composition of Coagulation-elements in Cumulonimbus, Quart. Jour. Roy. Met. Soc., v. 76, 1952, p.543-553.

Macky, W. A., Some Investigations on the Deformation and Breaking of Water Drops in Strong Electric Fields, Proc. Roy. Soc. London, Series A, v. 133, 1931, p.565-587.

_____, The Deformation of Soap Bubbles in Electric Fields, Phil. Soc. Proc., v. 26, Pt.3, 1930, p.421-428.

Mason, B. J., and J. Maybank, The Fragmentation and Electrification of Freezing Water Drops, Quart. Jour. Roy. Met. Soc., v. 86, 1960, p.176-185.

Marshall, J. S., and R. H. Margarvey, "Heat Transfer From Falling Water Drops", U.S. Air Camb. Res. Cen., #13, May 1952, p.91-100.

Nolan, J. J., The Breaking of Water-Drops by Electric Fields, Proc. Roy. Irish Acad., Sec.A, v. 37-38, 1926, p.28-39.

Reynolds, S. E., and M. Brook, Correlation of the Initial Electric Field and the Radar Echo in Thunderstorms, Jour. Met., v. 13, 1956, p.376-380.

Spilhaus, F. A., "Size, Shape, and Fall Speed of Raindrops", Jour. Met., v. 5, No.3, 1948, p.108-110.

Twomey, S., Electrification of Individual Cloud Drops, Tellus 8, 1956, p.445-452.

Vonnegut, B., C. B. Moore, and A. Botka, Preliminary Results of an Experiment to Determine Initial Precedence of Organized Electrification and Precipitation in Thunderstorms, Jour. Geophys. Res., v. 64, 1959, p.347-357.

Wilson, C. T. R., and G. I. Taylor, The Bursting of Soap-Bubbles in a Uniform Electric Field, Phil. Soc. Proc., v. 22, Pt. 5, 1924, p.728-730.

Workman, E. J., On Geochemical Effects of Freezing, Science, v. 119, No.3080, Jan. 8, 1954, p.73.

_____, M. Brook, and N. Kitagawa, Lightning and Charge Storage, Jour. Geophys. Res., v. 65, No.5, May 1960, p.1513-1517.

_____ and S. E. Reynolds, A Suggested Mechanism
for the Generation of Thunderstorm Electricity, The
Phys. Rev., v. 74, No.6, Sept. 15, 1948.

_____, Electrical Activity
as Related to Thunderstorm Cell Growth, Bul. Am. Met.
Soc., v. 30, 1949, p.142-144.

_____, Electrical Phenomena
Occurring During the Freezing of Dilute Aqueous
Solutions and Their Possible Relationship to
Thunderstorm Electricity, The Phys. Rev., v. 78, No.3,
May 1, 1950, p.254-259.

_____, Production of Electric
Charges on Water Drops, Nature, v. 169, June 28, 1952,
p.1108-1109.

_____, Structure and
Electrification, Thunderstorm Electricity, U. of Chicago
Press, 1953, p.139-149.

This thesis is accepted on behalf of the faculty of the
Institute by the following committee:

Max Brook

William D. Brozier

Martin S. Friberg

M. H. Wilkening

Ralph M. McGehee

Date: May 22, 1963